The role of the optic tectum for visually evoked orienting and evasive movements

Daichi G. Suzuki (鈴木 大地)[a,b], Juan Pérez-Fernández[a], Tobias Wibble[a,c], Andreas A. Kardamakis[a], and Sten Grillner[a,1]

[a]Department of Neuroscience, Karolinska Institutet, SE-171 77 Stockholm, Sweden; [b]Exploratory Research Center on Life and Living Systems (ExCELLS), National Institutes of Natural Sciences, Okazaki, 444-8787 Aichi, Japan; and [c]Division of Ophthalmology and Vision, Department of Clinical Neuroscience, Marianne Bernadotte Centre, Karolinska Institutet, SE-171 77 Stockholm, Sweden

Contributed by Sten Grillner, June 11, 2019 (sent for review May 8, 2019; reviewed by Ansgar Büschges and Réjean Dubuc)

As animals forage for food and water or evade predators, they must rapidly decide what visual features in the environment deserve attention. In vertebrates, this visuomotor computation is implemented within the neural circuits of the optic tectum (superior colliculus in mammals). However, the mechanisms by which tectum decides whether to approach or evade remain unclear, and also which neural mechanisms underlie this behavioral choice. To address this problem, we used an eye–brain–spinal cord preparation to evaluate how the lamprey responds to visual inputs with distinct stimulus-dependent motor patterns. Using ventral root activity as a behavioral readout, we classified 2 main types of fictive motor responses: (*i*) a unilateral burst response corresponding to orientation of the head toward slowly expanding or moving stimuli, particularly within the anterior visual field, and (*ii*) a unilateral or bilateral burst response triggering fictive avoidance in response to rapidly expanding looming stimuli or moving bars. A selective pharmacological blockade revealed that the brainstem-projecting neurons in the deep layer of the tectum in interaction with local inhibitory interneurons are responsible for selecting between these 2 visually triggered motor actions conveyed through downstream reticulospinal circuits. We suggest that these visual decision-making circuits had evolved in the common ancestor of vertebrates and have been conserved throughout vertebrate phylogeny.

visuomotor transformation | superior colliculus | evolution

All freely moving animals need to escape from predators or avoid obstacles as they move around and, at the same time, be able to orient toward objects of interest, as during foraging. It is thus critical to quickly detect and interpret surrounding events by integrating multisensory inputs to produce appropriate sensorimotor responses. In all vertebrates, the optic tectum (the superior colliculus in mammals) is central for visuomotor transformation (1–4). This brain region is conserved throughout vertebrate phylogeny (5), and is already well-developed in the adult lamprey, which belongs to the oldest group of now-living vertebrates (i.e., cyclostomes) that diverged 560 million years ago (6) from the evolutionary line leading up to mammals. The emergence of the optic tectum is linked to the evolution of image-forming vision, and contributed to the evolutionary success of vertebrates (7–10). Establishment of the neural circuits responsible for visual decision making at the level of the optic tectum represents a behavioral innovation and an important evolutionary event (11).

As in other vertebrates, the optic tectum of the lamprey has a retinotopically arranged visual map on the surface (12) and an underlying motor map controlling eye and orienting movements (13). The optic tectum has 3 major layers (Fig. 1): the superficial layer, intermediate layer, and deep layer (14, 15). The superficial layer receives retinal afferents conveying visual information from the surrounding space (12, 14), while the intermediate and deep layers receive similar spatial information via electrosensory afferents from the octavolateral area. Neurons in the deep layer integrate information from both senses via their dendrites that extend into the superficial and intermediate layers (12, 14). In addition, pallium (cortex in mammals) contributes with monosynaptic glutamatergic input to the neurons of tectum (16), while the output nuclei of the basal ganglia instead provide tonic gamma-aminobutyric acid (GABAergic) inhibition as in mammals (16, 17). These different inputs are integrated in tectum, and the tectal circuitry itself can select between eliciting an orienting or an evasive motor command (14, 18). The deep layer contains 2 types of output neurons: the contralateral brainstem-projecting (coBP) neurons that generate orienting movements and the ipsilateral brainstem-projecting (iBP) neurons that evoke evasive movements, as when avoiding obstacles (Fig. 1). The iBP neurons are distributed uniformly in all parts of the retinotopic map in tectum, while the coBP neurons are located primarily in the area that receives visual information from locations in front of the animal (12, 14). In the superficial layer, there are also GABAergic inhibitory interneurons activated by retinal afferents. They are sparsely distributed in the superficial and intermediate layers and contribute to stimulus selection via global (lateral) and local feed-forward inhibition of deep layer output neurons, both for unimodal visual stimuli (14) and for multimodal interplay (e.g., between visual and electrosensory stimuli) (15). In mammals, the responses to stimuli from the surrounding space often result from visual and/or auditory signals (3). Depending on the species, certain visual stimuli generate specific motor responses. In mice, an overhead visual stimulus increasing rapidly in size (an approaching predator) evokes a flight response, while a slowly moving visual stimulus (a cruising predator) induces a freezing response (19). In zebrafish, on the other hand, slowly moving dots, similar to the microorganisms they feed on, evoke approaching behavior, while looming stimuli (predator-like) induce escape swimming. Also, in invertebrates like the fruit fly, it has been shown that looming stimuli generate escape responses that drive the flies to take off via feature-detecting neurons (20). In both mice (21)

Significance

The optic tectum (the superior colliculus in mammals) is central for visuomotor transformation in all vertebrates. Here, we investigate the mechanisms underlying the selection between approaching and evasive movements. We use an isolated eye–brain–spinal cord preparation from the lamprey that allows us to display different types of visual stimuli (e.g., looming stimuli) and, at the same time, record neural activity from specific brain regions and the behavioral output monitored through the ventral roots. We show that 2 classes of brainstem-projecting neurons in the deep layer of tectum, in interaction with local inhibitory interneurons, are responsible for the selective switch between visually triggered approaching or evasive movements. We suggest that these visual decision-making circuits are phylogenetically conserved throughout vertebrate evolution.

Author contributions: D.G.S., J.P.-F., A.A.K., and S.G. designed research; D.G.S., J.P.-F., and T.W. performed research; D.G.S. analyzed data; and D.G.S., J.P.-F., and S.G. wrote the paper.

Reviewers: A.B., University of Cologne; and R.D., Université du Québec à Montréal.

The authors declare no conflict of interest.

Published under the PNAS license.

[1]To whom correspondence may be addressed. Email: sten.grillner@ki.se.

This article contains supporting information online at www.pnas.org/lookup/suppl/doi:10.1073/pnas.1907962116/-/DCSupplemental.

Published online July 11, 2019.

Downloaded at Palestinian Territory, occupied on November 26, 2021

www.manaraa.com

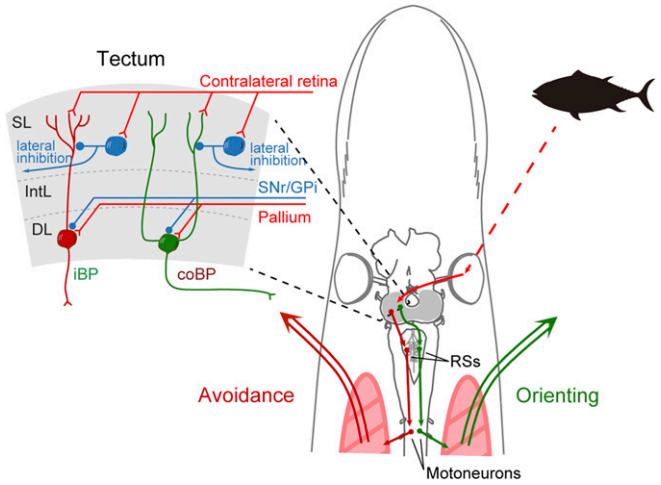

Fig. 1. Tectal neural circuits for visual behavior. (*Left*) Optic tectum has 3 main layers. Visual inputs from the contralateral retina target the superficial layer (SL), where most GABAergic interneurons (blue) are sparsely distributed. The intermediate layer (IntL) receives inputs from other brain centers, including the substance nigra pars reticulata (SNr), globus pallidus interna (GPi), and pallium. In the deep layer (DL), there are contralaterally and ipsilaterally brainstem-projecting neurons (coBP and iBP, respectively). (*Right*) In the lamprey, visual information (a fish silhouette here) selectively activates coBP or iBP neurons, which elicit muscle contraction on each side via reticulospinal neurons (RSs) and spinal motoneurons, resulting in orienting or avoidance movement, respectively.

and zebrafish (22, 23), these behaviors are thought to be controlled by the optic tectum. These studies suggest that such behavioral switches are dependent on the kind of stimuli the optic tectum receives, but its stimulus–response relationships are unknown.

Our primary aim here is to investigate the properties of the visual stimuli and the neural circuits that generate opposing orienting or evasive movements, and when the switch occurs. For this purpose, we used a unique "isolated eye–brain–spinal cord" preparation (14), which allowed us to apply different visual stimuli while recording from the optic tectum, reticulospinal neurons, and the ventral roots. Ventral roots innervate trunk muscles, and their activation will thus generate a motor response. Alternation of activity between motoneurons on the right and left sides generates swimming (24). On the other hand, steering movements are produced by asymmetrical activation of reticulospinal neurons, which, in turn, evokes larger ventral root bursts on the side toward which a turning response is produced (24–26). Accordingly, when this mechanism is modeled and implemented in a robotic model, appropriate orienting and evasive movements are generated (27). Thus, recording activity in the ventral roots on the side where the stimulus is presented can be interpreted as an orienting movement, whereas activation of the contralateral side can be interpreted as an evasive movement. Slow looming stimuli evoke activity selectively in ventral roots on the same side, corresponding to orienting movements, which become larger when the stimuli are applied in the visual field in front of the animal. On the other hand, rapidly expanding looming stimuli that could be perceived as threatening tend to induce strong bilateral burst responses in the ventral roots, as in fast evasive movement or rapid escape. The stimulus-type selectivity was abolished when tectal GABAergic interneurons were inactivated pharmacologically. The visuomotor responses in the ventral roots were disrupted by blocking the activity of the tectal deep layer or the downstream reticulospinal neurons, showing that tectum and the reticulospinal transmission are critical.

Results

The Characteristics of the Visual Stimulus Determine the Motor Response. To evaluate the stimulus–response relationships, we provided different types of visual stimuli presented through a computer screen in front of the eye of an "isolated eye–brain–spinal cord preparation" (Fig. 2*A* and *Materials and Methods*). The efferent motor response was recorded from the ventral roots in the rostral spinal cord, and activity in other areas related to visuomotor processing, including tectum or reticulospinal neurons, was recorded to analyze their contribution to the evoked motor responses. With this experimental approach, we could present to the animal a wide range of visual stimuli, for example, horizontally moving vertical bars and looming dots expanding with different speeds.

Orienting responses. As shown in Fig. 2*B* (also Movie S1), a "slow looming stimulus" elicited a response in the left optic tectum (contralateral to the stimulated eye, black trace) and a marked activation of the right ventral root (ipsilateral to the stimulated eye, green trace), but only a modest activation on the left side (left ventral root; red trace). The ipsilateral ventral root activation would have resulted in an orienting movement. To analyze the evoked responses, we quantified the number of spikes and analyzed the spiking patterns (n = 20 trials from 11 lampreys) with raster plots (Fig. 2*C*) and with peristimulus time histograms (PSTHs; Fig. 2*D*). There is a clear difference between the ipsilateral right side (green, Fig. 2*D*) and the response on the left side (red, Fig. 2*D*), which also shows that the peak response occurs during the growing phase. The looming stimuli used in Fig. 2 *B–D* expanded linearly (3.5-cm·s^{-1} increase in diameter). However, when an object approaches the eye with constant speed, it will instead increase quasiexponentially in size. Therefore, we tested the effect of slow "exponential" looming stimuli (Fig. 2*E*) and showed that there also is a marked difference between the 2 sides (n = 10 from 5 lampreys) in this case, with a prominent orienting-like response. This is also clear from the quantification of the spike counts shown in Fig. 2*K*, which reinforce the difference for both linear and exponential slow looming stimuli. The right (orienting) side also responded faster than the left side (Fig. 2*L*), further reinforcing that slow looming stimuli evoke orienting responses.

Evasive responses. When fast looming stimuli (linear or exponential) were applied, a strong tectal response and bilateral ventral root activation occurred, often strongest on the left "evasive" side (Fig. 2 *F–H* and Movie S2; n = 27 from 12 lampreys for linear stimuli and n = 12 from 6 lampreys for exponential stimuli), as is evident from PSTHs in Fig. 2 *G* and *H* (also Fig. 2 *K* and *L*). A similar response was observed when we applied a vertical bar (black on white background) moving horizontally (Fig. 2 *I* and *J*). "Bar R to C" (moving rostral to caudal) tended to activate the ventral root on the evasive left side more than on the right side (Fig. 2 *I* and *K*; n = 16 from 10 lampreys), while "bar C to R" (moving caudal to rostral) evoked ventral root activity on both sides in a more symmetrical manner (Fig. 2 *J* and *K*; n = 21 from 11 lampreys). Taken together, we found that threatening-like stimuli (bars and fast looming) tended to activate the evasive left side stronger and faster than the right side (*SI Appendix*, Table S1). This was clearer for "bar R to C" than for the other cases, implying that "bar R to C" elicits a stronger avoiding response, whereas the others tend to evoke escaping forward responses. We confirmed this interpretation by monitoring the behavioral responses in an intact animal, which showed evasive head movements for "bar R to C" and a strong swimming response to "bar C to R" (Movie S3). These responses are ethologically relevant to avoid collisions with obstacles in front and to escape from objects approaching from behind. Our results suggest that naturally threatening-like stimuli such as fast looming dots or horizontally moving bars will elicit evasive-like or rapid escape-like behavior in contrast to slow looming stimuli.

The Optic Tectum Shows Different Responses to Various Visual Stimulus Properties.

Speed. The distinct responses generated by fast and slow looming stimuli, respectively, showed that the speed of change of the visual stimuli determines the motor activity generated. We therefore measured the field potential in the deep layer of tectum in response

Downloaded at Palestinian Territory, occupied on November 26, 2021
www.manaraa.com

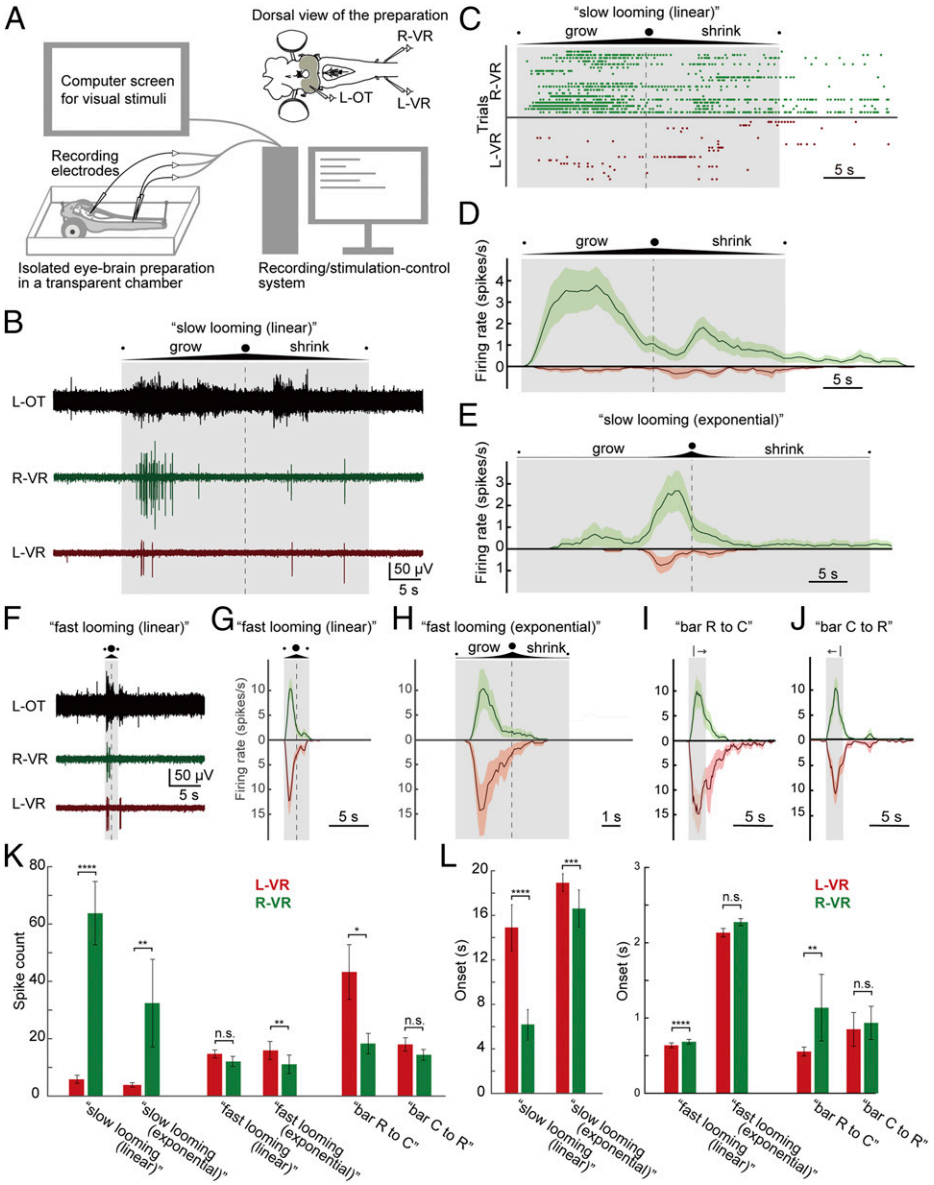

Fig. 2. Motor response to looming/bar visual stimuli applied at different speeds. (*A*) Schematic illustration of the experimental system. (*Top Right*) Isolated eye–brain preparation was placed in a cooling chamber perfused with aCSF, and neural activity was recorded from the left optic tectum (L-OT) and ventral roots on both sides (left ventral root [L-VR] and right ventral root [R-VR]). A computer screen for presenting visual stimuli was placed on the right side of the preparation connected to a computer, which was used to synchronously control the recordings and the visual stimulation. (*B*) Tectal and ventral root activity evoked by the "slow looming (linear)" visual stimuli (a looming dot on white background, linearly expanding to cover the entire screen at the maximum limit and then shrinking at 3.5 cm·s^{-1}). The duration of the stimulus and the point of maximum expansion are shown by a shaded box and a dashed line, respectively. Note that the ventral root on the orienting right side (green) is more strongly activated, compared with the left side (red). (*C*) Raster plots for "slow looming (linear)" showing the evoked spikes in the ventral roots over time for 20 trials. (*D*) PSTH for "slow looming (linear)" stimuli showing spike probability through time, combining data from the raster plots. Data are represented as mean ± SEM. (*E*) PSTHs for "slow looming (exponential)" based on 10 trials. Here "exponentially" growing (and shrinking) dots are used to simulate a situation where a circular project approaches the eye with constant speed (the diameter of the circle increases/decreases 1.35-fold per second). Similar to the "slow looming (linear)," "slow looming (exponential)" stimuli also preferentially evoke ventral root activity on the orienting right side (green). (*F*) Tectal and ventral root activity evoked by "fast looming (linear)" visual stimuli, 10-fold faster than "slow looming (linear)" (i.e., growing and shrinking 35 cm·s^{-1} on the screen). (*G*) PSTHs for "fast looming (linear)" visual stimuli based on 27 trials. Note that the ventral roots on both sides are activated. (*H*) PSTHs for "fast looming (exponential)" stimuli (the diameter of the circle increases/decreases 18.7-fold per second) based on 10 trials. Likewise, the ventral roots on both sides are activated. (*I* and *J*) PSTHs for visual stimuli consisting of black vertical bars moving from rostral to caudal (based on 16 trials) or from caudal to rostral (21 trials) with respect to the animal (with a total stimulus duration in both cases of 2.1 s). (*I*) When the bar moves rostral to caudal ("bar R to C"), it tends to activate the ventral roots on the evasive left side more than on the right orienting side. (*J*) On the other hand, when the bar moves caudal to rostral ("bar C to R"), it evokes ventral root activity on both sides in a more symmetrical manner. (*K*) Plots showing the average spike counts from L-VR and R-VR, respectively, for "slow looming (linear)," "slow looming (exponential)," "fast looming (linear)," "fast looming (exponential)," "bar R to C," and "bar R to C" stimuli (also *SI Appendix*, Table S1). Data are represented as mean ± SEM. Slow looming stimuli evoke significantly more spikes in the ventral root on the (orienting) right side than on the left side. On the other hand, threatening-like stimuli (fast looming dots and bars) tend to activate the evasive left side stronger than the right side. (*L*) Plots showing the average onset. Data are represented as mean ± SEM (*P* values are provided in *SI Appendix*, Table S1). Note that different scales are used between slow looming stimuli and the others. Slow looming stimuli evoke spikes on the orienting right side significantly earlier than on the left side, while threatening-like stimuli tend to elicit activity on the evasive left side earlier than on the right side. *$P < 0.05$, **$P < 0.01$, ***$P < 0.001$, ****$P < 0.0001$. n.s., no statistical significance.

Downloaded at Palestinian Territory, occupied on November 26, 2021
www.manaraa.com

to looming stimuli (linearly growing/shrinking [i.e., at constant speed]) at 6 different speeds (Fig. 3*A*), from a slow looming speed (linear) of 3.5 cm·s^{-1} (on the screen) to a 100-fold faster looming (350 cm·s^{-1}; $n = 10$ for each stimulus from 3 lampreys). The results show that faster looming stimuli evoked larger tectal local field potentials (LFPs; reflecting population activity of the deep layer tectal neurons), and that the duration of the tectal response decreased markedly. The graph in Fig. 3*B* shows a striking log-linear correlation ($R^2 = 0.99972$) between the amplitude of tectal responses and the relative speed of the looming stimulus.

Contrast. We then tested responses to different object/background contrast. We changed gray levels (100% = black, 0% = white) of the object on a white background, using "fast looming (linear)" ($n = 10$ for each gray level from 3 lampreys). As a result, stronger LFPs from the deep layer of tectum were observed when higher contrast (darker gray) stimuli were applied (Fig. 3*C*), also with clear log-linear correlation ($R^2 = 0.79839$) between the peak amplitude and gray level (Fig. 3*D*). The same tendency was found after comparing normalized integral LFPs (*SI Appendix*, Fig. S1), although the correlation is weaker than the peak amplitudes. It is also notable that a very light gray looming stimulus (1.6% in grayscale) was sufficient to induce tectal activity, although with a longer latency and smaller amplitude. This finding indicates that the visual system of the lamprey is quite sensitive to contrast.

Color. To explore whether wavelengths (colors) matter in the observed sensory stimulation paradigm, "fast looming (linear)" stimuli were applied in 3 different colors (red, green, and blue [RGB]; the primary colors in the RGB color model used for liquid crystal display [LCD] monitors; *Materials and Methods*) on a white background ($n = 10$ for each stimulus from 3 lampreys). LFPs from the tectal deep layer were observed for all 3, with no significant differences in maximum amplitude (Fig. 4 *A* and *B*), although the blue stimuli tended to evoke the largest responses and the green stimuli the smallest (Fig. 4*B*).

To test whether contrast (Fig. 3 *C* and *D*) is important in this context, a gray-scaled background was used to constrain our parameter space (blue is the darkest primary color and green the lightest) with the same brightness as the color of the stimulus (for brightness adjustment; *Materials and Methods*). Even on this background, all 3 colors evoked similar responses (Fig. 4*C*). The maximum amplitude was, however, more similar than on white background (compare Fig. 4 *B* and *D*). These results suggest that the lamprey can distinguish colors from a gray-scaled monochrome background (*Discussion*).

Visual Objects Located in the Anterior Visual Field Enhance Orienting Behavior. We then tested the visual field dependency of the visually evoked motor response. For this, we used small "slow looming (exponential)" stimuli, expanding maximally to one-fourth of the screen, applied in 8 different positions (Fig. 5*A*).

The response of the ventral root on the orienting right side was significantly larger when we applied the stimulus in the rostral visual field (Fig. 5 *B* and *E*), compared with the response for a stimulus in the caudal visual field (Fig. 5 *C* and *E*; $P = 0.0073$; $n = 9$ from 3 lampreys). The polar plots showing the firing rate for identical stimuli in each of the applied positions indicate that this enhancement is the strongest when the stimulus is applied in the rostral visual field (Fig. 5*D*, R-VR). This finding agrees with the fact that the majority of coBP neurons are found in the rostral area of the optic tectum that is the recipient of synaptic inputs from the posterior retina (12, 14), from which orienting-like movements can be elicited by electric stimulation (13). Taken together, these results suggest that the likelihood to evoke orienting movements is higher when the target object is located in the rostral visual field. The response in the left ventral root is much smaller than in the right ventral root (Fig. 5 *D* and *E*), and there is no significant difference between rostral or caudal stimuli (Fig. 5*E*, *Right*; $P = 0.3255$).

Tectal Microcircuits Mediate the Orienting and Evasive Motor Responses. To verify that the effects observed are mediated via tectum, we interfered with tectal function pharmacologically. Different drug injections were performed in tectum (contralateral to the screen; *Materials and Methods*), aiming at affecting the entire tectum, while ensuring that adjacent areas were not affected. We used "fast looming (linear)" stimuli since they generate a symmetrical strong response in the ventral roots of both sides mediated by both coBP and iBP neurons. The nonselective glutamate receptor antagonist kynurenic acid (Fig. 6*A*) was microinjected (*Materials and Methods*) in several locations into the optic tectum to block excitatory synaptic transmission from the retinal afferents to the coBP and iBP neurons. After the injections, the responses to a fast looming stimulus were practically abolished in both ventral roots (Fig. 6 *B* and *C*; $P = 0.001$, control vs. injection; $n = 14$ from 3 lampreys). The same was observed when 2-aminophosphono-5-valeric acid (AP5) or 2,3-dioxo-6-nitro-1,2,3,4-tetrahydrobenzo[f]quinoxaline-7-sulfonamide (NBQX) was applied to selectively remove the *N*-methyl-D-aspartate (NMDA) and α-amino-3-hydroxy-5-methyl-4-isoxazolepropionic acid (AMPA) components, respectively. Both reduced markedly the evoked response (*SI Appendix*, Fig. S2 *B* and *C*; $n = 13$ [AP5] from 3 lampreys and $n = 14$ [NBQX] from 3 lampreys), indicating that the synaptic effects are mediated via both NMDA and AMPA receptors (14). Similarly, when the neuronal transmission in tectum was blocked by injection of the sodium channel blocker tetrodotoxin (TTX; *SI Appendix*, Fig. S2*A*; $n = 6$ from 3 lampreys), the response was abolished.

To remove the GABAergic inhibition in the tectal microcircuits (14, 15) gabazine was microinjected (Fig. 7*A*), which caused a drastic enhancement of the evoked ventral root activity on both sides, abolishing any dependence on the stimulus applied (Fig. 7 *B*–*E*). For example, the "slow looming (linear)" stimulus elicited ventral root activity only on the orienting right side before gabazine injection, but both sides were strongly activated after the injection (Fig. 7*E*; $n = 8$ from 3 lampreys). These results suggest that the engagement of the local inhibitory networks contributes not only to stimulus selection but also to selection of motor action (also Fig. 1).

Tectal Effects Are Mediated via Reticulospinal Neurons. Major targets of the tectal motor commands are the middle rhombencephalic reticulospinal nucleus (MRRN) (14, 18), which receives monosynaptic excitatory postsynaptic potentials (EPSPs) from the coBP and iBP neurons (on separate sides). To analyze whether reticulospinal neurons transmit the motor commands from tectal neurons to spinal motor neurons (Fig. 1), we simultaneously recorded extracellular neural activity in the MRRN and ventral roots bilaterally. Fig. 8*A* shows that reticulospinal neurons on both sides are active in phase with the motoneurons on the ipsilateral side and with precise timing (with an ∼2.4-ms delay) in response to the fast looming stimuli. To analyze the contribution of reticulospinal neurons in activating ipsilateral versus contralateral spinal motoneurons in response to visual stimuli (Fig. 8*B*), we injected muscimol (a GABA type A [$GABA_A$] agonist) locally in the MRRN. The extension of the injections into the MRRN (which is clearly visible) was monitored (*Materials and Methods*) so that the effect of muscimol was limited to the ipsilateral side. Injections on the left side abolished the ventral root activity mainly on the same left side ($P = 0.0033$, the right ventral root vs. the left ventral root), and a subsequent injection on the right side abolished the response on that side ($n = 7$ from 3 lampreys). These findings show that neurons in the MRRN mediate the tectal responses to their downstream ipsilateral spinal motoneurons.

To analyze the contribution of individual reticulospinal neurons in generating orienting and evasive responses, we performed intracellular recordings in either the left or right MRRN. Reticulospinal neurons on both the left and right sides were responsive to "fast looming (linear)" stimuli (Fig. 8*C*). Interestingly, all neurons ($n = 6$ of 6) which responded to the "fast looming

Downloaded at Palestinian Territory, occupied on November 26, 2021
www.manaraa.com

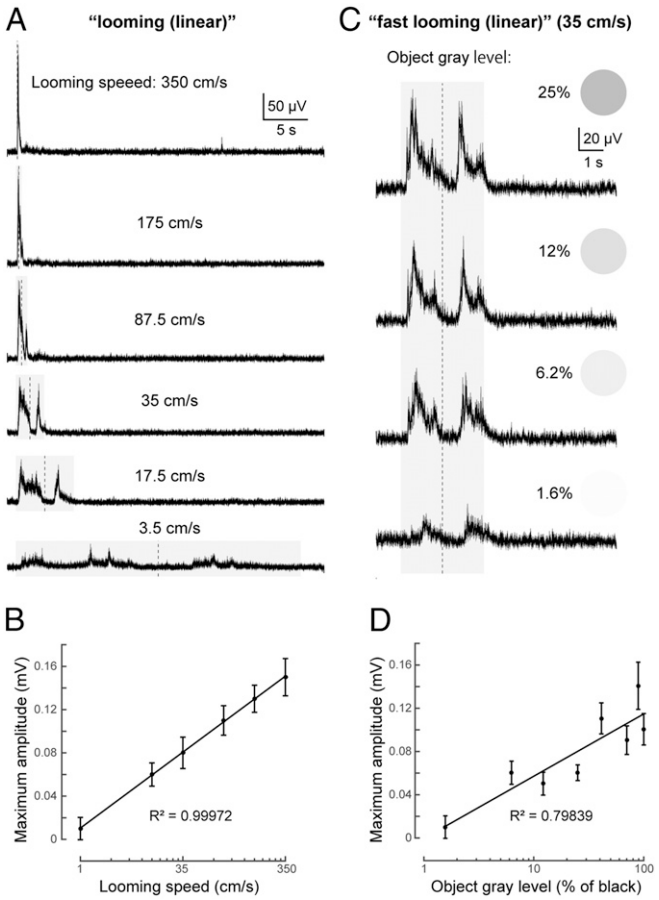

Fig. 3. Tectal responses to looming stimuli at different speeds and contrast. (*A*) Averaged (10 trials each) LFPs recorded from the deep layer of tectum for "looming" (linear) stimuli at different speeds, from 3.5 to 350 cm·s^{-1}. Stimulus duration is shown by the shaded area, and the vertical dotted line shows the point of maximum expansion. (*B*) Graph showing the strong log-linear correlation between maximum amplitude of LFPs and relative speed. Data are represented as mean ± SEM. (*C*) Averaged (of 10 trials each) tectal LFPs evoked by "fast looming (linear)" stimuli (35 cm·s^{-1}) with different levels of gray (1.6%, 6.2%, 12%, and 25%; with 0% being white and 100% black). Averaged LFPs in response to a black looming stimulus (100% gray) with the same speed (35 cm·s^{-1}) can be seen in Fig. 3*A*. (*D*) Graph showing the log-linear correlation between maximum amplitude of LFPs and the object gray level. Data are represented as mean ± SEM.

(linear)" stimuli on the orienting right side also responded to "slow looming (linear)" stimuli, whereas "fast looming" stimuli-responsive neurons on the left side rarely responded to the "slow looming (linear)" stimuli (n = 2 of 7). This further supports the notion that "slow looming" stimuli activate primarily coBP neurons, and thus reticulospinal neurons, on the orienting right side (contralateral to the left visually stimulated tectum).

Discussion

In this study, we have employed the unique isolated eye–brain preparation of the lamprey to investigate visuomotor transformation. This has allowed us to display different types of visual stimuli and explore the effects in terms of the neural correlates of orienting and evasive behavior, while investigating the intervening processing in tectum and the reticulospinal nucleus, MRRN. The accessibility of the eye–brain preparation has allowed us to apply behavioral, pharmacological, and intra- and extracellular techniques.

Slow looming dots activate preferentially the ventral root ipsilateral to the side of the visual stimulus, representing orienting-like behavior. Threatening-like visual stimuli such as a horizontally moving bar and fast looming dots tend to evoke burst responses in ventral roots on both sides, reminiscent of evasive movement or rapid escape. These visual responses are processed in tectum, since they were abolished by selectively blocking glutamatergic transmission in tectum and disrupted by silencing GABAergic neurons in the tectal superficial layer. There are 2 types of glutamatergic neurons in the tectal deep layer: coBP neurons activating contralateral reticulospinal neurons and iBP neurons activating reticulospinal neurons on the ipsilateral side (14). These 2 types of tectal output neurons send motor commands to respective sides of the brainstem, where reticulospinal neurons transmit the commands to spinal motoneurons (Fig. 1). Our results support the notion that preferential activation of coBP neurons elicits orienting movements, while iBP neurons trigger evasive movements, depending on the characteristics of the visual stimuli (type, position, etc.). Pretectal neurons can also excite

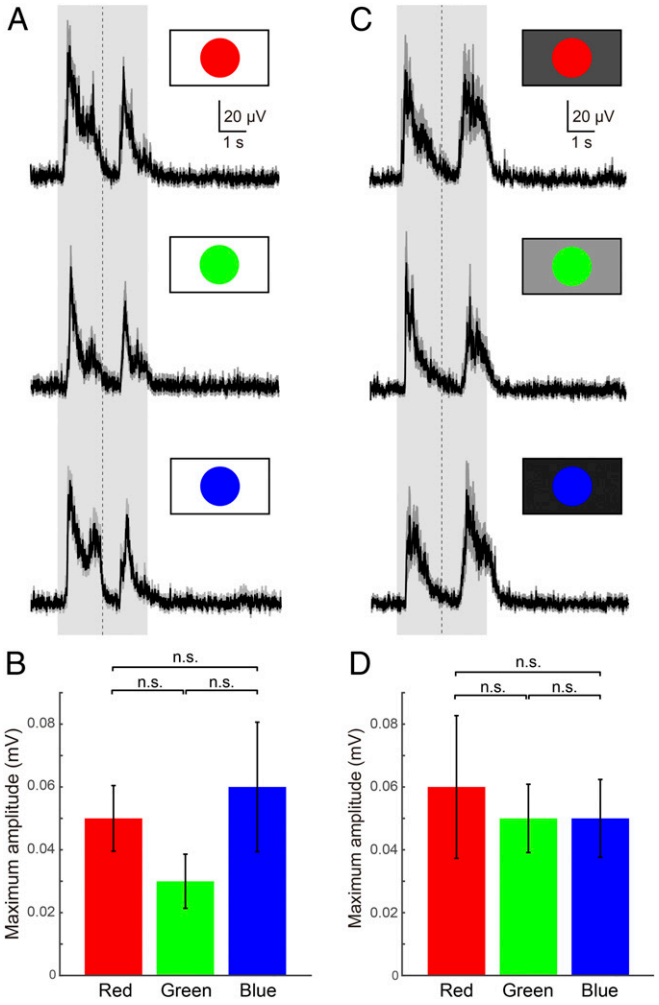

Fig. 4. Tectal responses to looming stimuli of different colors. (*A*) Averaged (10 trials each) tectal LFPs in response to red, green, and blue "fast looming (linear)" visual stimuli on a white background. The shaded area indicates the duration of the stimulus, and the vertical dotted line indicates the point of maximum expansion. (*B*) Plots showing the average maximum amplitude of LFPs. Data are represented as mean ± SEM (P = 0.3679). (*C*) Averaged (10 trials each) tectal LFPs for red, green, and blue "fast looming (linear)" visual stimuli on a brightness-adjusted background (*Material and Methods*). (*D*) Plots showing the average maximum amplitude of LFPs, demonstrating that all colors can be distinguished from backgrounds with the same brightness. Data are represented as mean ± SEM (P = 0.8700). n.s., no statistical significance.

Downloaded at Palestinian Territory, occupied on November 26, 2021
www.manaraa.com

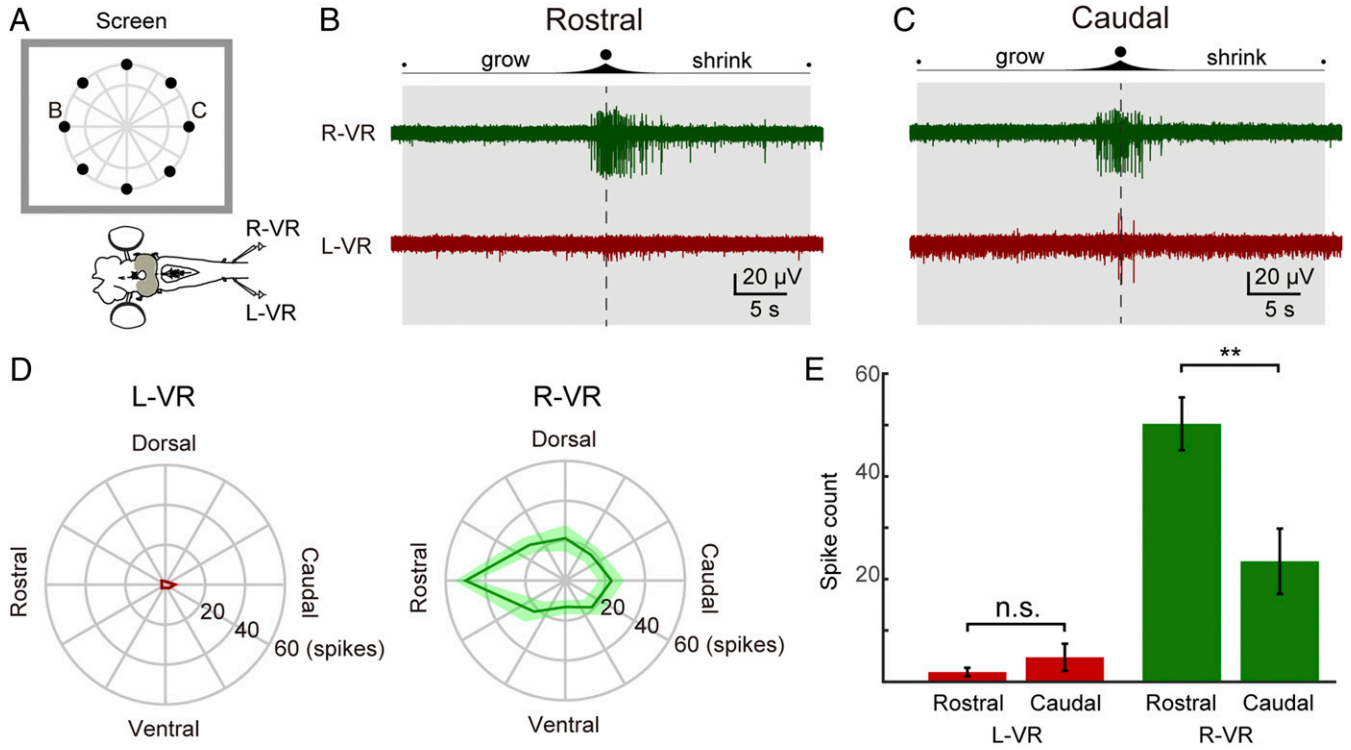

Fig. 5. Anterior visual field evokes the strongest orienting-like response. (*A*) Schematic illustration showing the 8 positions in which the "slow looming (linear)" stimuli were presented. The evoked motor outputs were monitored by recordings from the left and right ventral roots (L-VR and R-VR, respectively). (*B*) Representative response to a stimulus presented in a rostral position. The duration of the stimulus and the moment of maximum expansion are indicated by a shaded area and a vertical dotted line, respectively. Strong activity was observed in the R-VR (green trace), whereas no activity was detected in the L-VR (red trace). (*C*) Representative response to a stimulus presented in a caudal position. Compared with rostral stimuli, less activity was evoked in the R-VR (green trace), whereas more activity was evoked in the L-VR (red trace) compared with rostrally evoked responses. (*D*) Polar plots showing L-VR and R-VR average firing counts for each of the 8 positions. (*E*) Plots showing the average spike counts (of 9 trials) from the L-VR (*Left*, red) and R-VR (*Right*, green) in response to rostral and caudal visual stimuli, showing that rostral visual stimuli evoke activity on the orienting right side is significantly stronger than for caudal stimuli. Data are represented as mean ± SEM ($P = 0.3255$ for L-VR, $P = 0.0073$ for R-VR). n.s., no statistical significance.

reticulospinal neurons and are known to mediate the dorsal light response and negative phototaxis (11, 28–31), but they will not contribute to the effect of looming stimuli.

The Stimulus-Type Dependency and Tectal Neuron Activation. A slow looming stimulus that gives rise to an orienting behavior leads to a much smaller neuronal response in tectum than fast looming stimuli that result in evasive-like movements (Fig. 3*A*). Why are coBP neurons activated at a lower threshold than iBP neurons? One important difference is that the firing threshold is lower for coBP neurons than for iBP neurons (14). In other words, coBP neurons would be activated by weak stimuli that would be subthreshold for the iBP neurons. Fast looming stimuli, on the other hand, elicit a larger neural response in the tectal deep layer (Fig. 3 *A* and *B*) that will then include iBP neurons and issue an evasive response. Our results also show that the evoked responses in tectum to looming stimuli increase with the duration of the stimulus (Fig. 3*A*). This result can be explained by taking into account the retinotopic nature of tectum and the feedforward inhibition evoked by visual stimuli (14, 15). As a looming dot expands on the screen, new areas of tectum are activated, while recruited inhibition silences active regions. Fast stimuli will activate larger areas of tectum before being silenced by inhibition, generating a short peak of activity with large amplitude (Fig. 3*A*, top traces). For intermediate speed looming stimuli, 2 peaks of activity are evoked in response to expansion and shrinking, whereas for low speed looming stimuli, a slow activation of neurons takes place, which allows the inhibitory system to reset active areas, avoiding excitatory inputs to summate.

Another factor that may contribute to the stimulus selectivity is the GABAergic system. Tectal GABA interneurons have both local and long-range inhibitory projections. ON-receptive field retinal stimuli result in local excitation followed by feedforward inhibition, while OFF-field retinal stimulation evokes only lateral inhibition (14, 15). As we have shown, blocking GABAergic transmission results in drastically enhanced visual responses in the tectum and the ventral roots and in the loss of stimulus-type dependency (Fig. 7), providing evidence that the tectal GABAergic system is critical for the stimulus selection.

Dependency of Orienting Responses on the Visual Field. The orienting response evoked by "slow looming" stimuli is enhanced when the stimuli are shown in the anterior visual field (Fig. 5). This can be accounted for by the fact that coBP neurons are preferentially located in the anterior tectum (14), which represents the retinorecipient area for the anterior visual field (12). On the other hand, iBP neurons are evenly distributed over the retinotopic map (14) and can elicit evasive responses. Furthermore, we show that a horizontally moving bar elicits stronger avoidance responses when it moves from anterior to posterior in the visual field, while escape forward responses appear when the bar moves from posterior to anterior (Fig. 2 *I* and *J* and Movie S3). In the lamprey, retinal ganglion cells targeting tectum are more abundant in the posterior part of the retina (anterior visual field), although the projection pattern differs somewhat between the different subtypes (12). Therefore, the lamprey will receive more detailed visual information from the anterior part than from other parts of the visual field, as a basis of visuomotor decision making between orienting and avoiding movements.

Downloaded at Palestinian Territory, occupied on November 26, 2021
www.manaraa.com

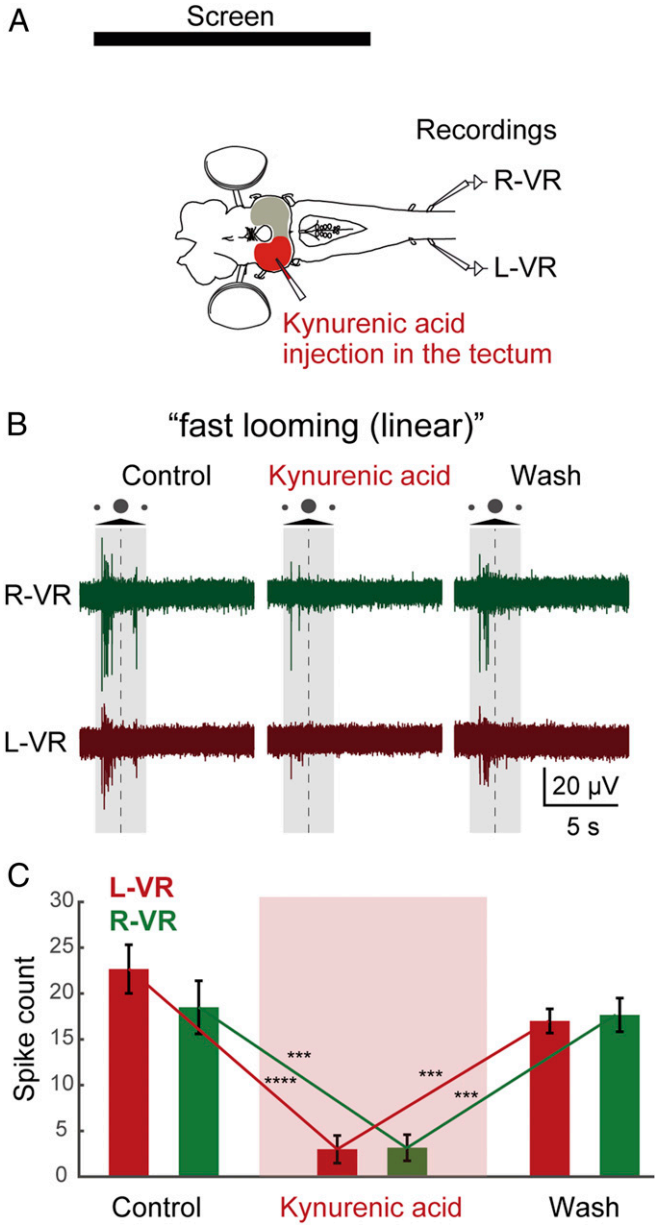

Fig. 6. Optic tectum mediates visually evoked ventral root responses. (*A*) Kynurenic acid injection in the optic tectum. L-VR, left ventral root; R-VR, right ventral root. (*B*) After kynurenic acid injection, motor responses to visual stimuli from both the L-VR and R-VR were totally abolished. The shaded area indicates the duration of the stimulus, and the dotted line indicates the moment of maximum expansion. (*C*) This observation is supported by the statistical analysis when comparing average spike counts (of 14 trials) from the L-VR and R-VR, between control and kynurenic acid ($P < 0.0001$ for L-VR, $P = 0.0004$ for R-VR) and kynurenic acid and washout ($P = 0.0003$ for L-VR, $P = 0.0007$ for R-VR). Data are represented as mean ± SEM. ***$P < 0.001$, ****$P < 0.0001$.

Processing and Modulation of Visual Stimuli. We found that the looming speed and brightness (or contrast between visual objects and the background) correlate logarithmically with the tectal response (Fig. 3 *A* and *B*). This result suggests that the Weber–Fechner law (i.e., the relationship between stimulus and perception is logarithmic) can be applied in this case in the lamprey, suggesting common neural substrates (32, 33).

The sensitivity to the visual stimuli can be controlled by several mechanisms, although the lamprey has neither intraocular muscles (34) nor a distinct ciliary ganglion-like structure (35), suggesting that there is no control of the luminous flux by the pupil. However, glutamatergic and GABAergic retinopetal projections from the mesencephalic tegmentum have been reported, presumably involved in enhancing or reducing the responsiveness of retinal ganglion cells (36–38). In addition, the tectal neurons receive a dopaminergic modulation from the substantia nigra pars compacta (SNc), and iBP and coBP cells express either dopamine D1 or D2 receptors, which can facilitate the response to visual stimuli (39, 40). Furthermore, the deep layer of tectum receives monosynaptic input from pallium and inhibition from the output nuclei of the basal ganglia (14, 15). Thus, visual signals can, in fact, be influenced by a variety of neural mechanisms through the entire process from the retina to the final motor output.

Color Vision in the Lamprey. The Southern Hemisphere lamprey *Geotria australis* has 5 visual opsins and 5 types of photoreceptors (41). Phylogenetic analysis indicates that the ancestral lamprey also had all 5 subtypes of visual opsins (41–43). On the other hand, the Northern Hemisphere lamprey species, including those used in this study (*Petromyzon marinus* and *Lampetra fluviatilis*), only have 2 visual opsins (rhodopsin [Rh1] and long-wave-sensitive [LWS] opsin) and 2 types of photoreceptors (short and long), which correspond to the gnathostome rod and cone photoreceptors, respectively (43, 44). This group of lampreys may be degenerate regarding the number of opsins. Nevertheless, the optical characteristics of the lens indicate that the Northern Hemisphere lamprey has well-focused color vision (45).

Our results suggest that the Northern Hemisphere lamprey has at least bichrome (black/white plus 1 color) vision (Fig. 4). This additional color is possibly in the green range, because the long-type (the cone type in gnathostomes) photoreceptor expresses LWS opsin with a maximal spectral sensitivity of 555 nm in *L. fluviatilis* (46). Even though this wavelength is close to the maximal spectral sensitivity of the short-type (the rod type in gnathostomes) photoreceptors expressing Rh1 (512 nm in *L. fluviatilis*) (46), our results indicate that the lamprey can respond to every primary color (red, green, and blue) without any significant difference of sensitivity, especially when the contrast is adjusted (Fig. 4).

Evolution of Visual Behavior in Vertebrates. The behavioral switch between orienting-like and evasive-like movements depending on the looming speed is consistent with the needs of the lamprey to approach objects of interest (e.g., for feeding) but to escape from alarming stimuli. Also, in larval zebrafish, faster looming evokes escape behavior with a higher probability (22, 23). On the other hand, the larval zebrafish shows a behavioral switch depending on the size of moving dots (47), which is also consistent with its ethology because the larval zebrafish feeds on microorganisms (e.g., paramecia), while it needs to escape from larger predators. In both cases, weaker (slow looming or small size) visual stimuli appear to evoke approaching or orienting behavior, while stronger (fast looming or large size) stimuli trigger escape or evasive movements. This implies, considering the conserved structure of the tectum (48), that the neural mechanisms for the behavioral switch found here may be conserved throughout vertebrate phylogeny.

Materials and Methods

Animals. Experiments were performed on 42 adult river lampreys (*L. fluviatilis*) and 96 young adult sea lampreys (*P. marinus*) of both sexes. The experimental procedures were approved by the local ethics committee (*Stockholms Norra Djurförsöksetiska Nämnd*) and were in accordance with *The Guide for the Care and Use of Laboratory Animals* (49). Animals were kept in aquaria with an enriched environment, and water was aerated and filtered continuously. During the investigation, every effort was made to minimize suffering and to reduce the number of animals used.

Experimental Preparation for Visual Stimulation. To allow for recordings in the tectum and ventral roots while applying visual stimuli, we developed a preparation exposing the brain and the rostral segments of the spinal cord, maintaining the eyes intact (40). For this, the animal was deeply anesthetized with MS-222 (100 mg/L; Sigma), and the dorsal skin and cartilage were removed to expose the brain and spinal cord. The viscera and all muscles were removed to avoid movements. The

Downloaded at Palestinian Territory, occupied on November 26, 2021
www.manaraa.com

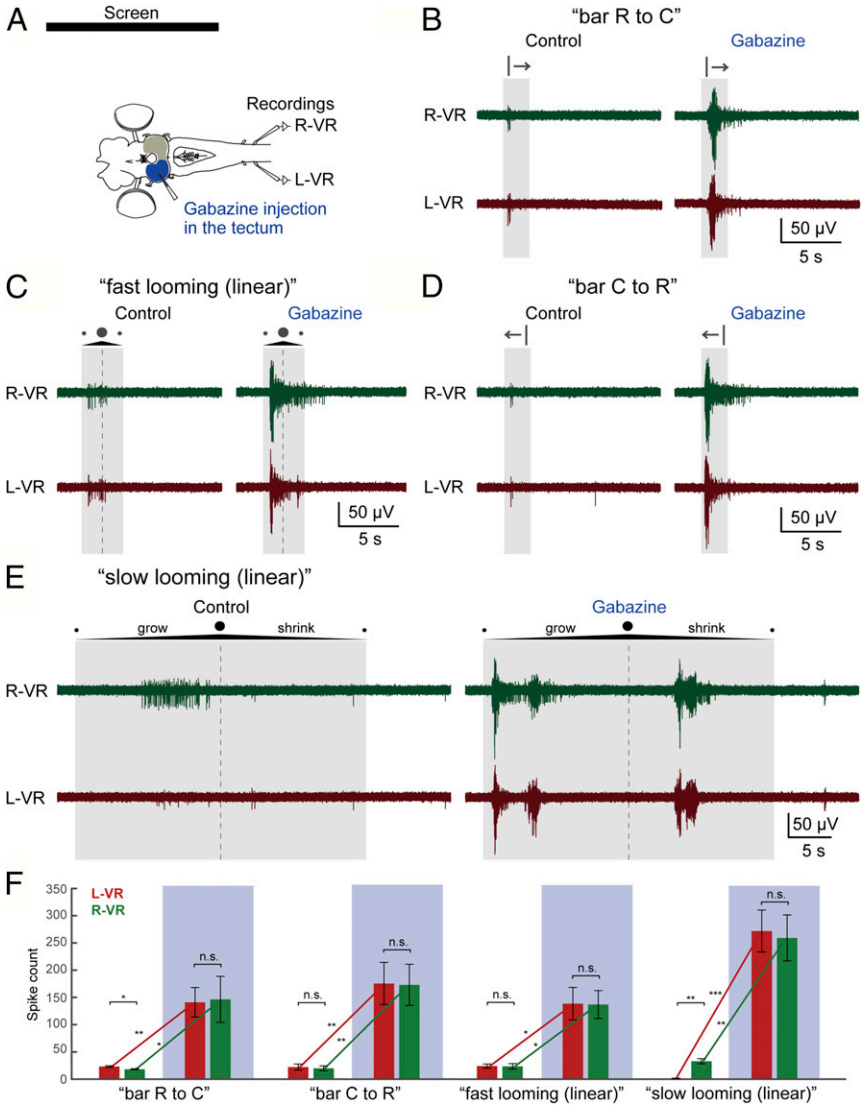

Fig. 7. Tectal inhibitory system contributes to the stimulus type-dependent motor responses. (*A*) Gabazine injection in the tectum. L-VR, left ventral root; R-VR, right ventral root. (*B–E*) After gabazine injection, drastic enhancement of the ventral root activity was observed on both sides, abolishing the stimulus-type dependency. Note that the "slow looming (linear)" stimulus strongly activates ventral roots on both sides after the gabazine injection. The shaded area and the dotted line show the duration of the stimulus and the moment of maximum expansion, respectively. (*F*) This observation is supported by the statistical analysis when comparing average spike counts (of 6 trials) from the L-VR (*Left*, red) and R-VR (*Right*, green) between control and gabazine injection (blue-shaded). Data are represented as mean ± SEM ("bar R to C": $P = 0.0136$ for L-VR vs. R-VR before injection, $P = 0.8326$ for L-VR vs. R-VR after injection, $P = 0.0068$ for before vs. after injection in L-VR, $P = 0.0285$ for before vs. after injection in R-VR; "bar C to R": $P = 0.3737$ for L-VR vs. R-VR before injection, $P = 0.7588$ for L-VR vs. R-VR after injection, $P = 0.0073$ for before vs. after injection in L-VR, $P = 0.0062$ for before vs. after injection in R-VR; "fast looming [linear]": $P = 0.8074$ for L-VR vs. R-VR before injection, $P = 0.8682$ for L-VR vs. R-VR after injection, $P = 0.0177$ for before vs. after injection in L-VR, $P = 0.0118$ for before vs. after injection in R-VR; "slow looming [linear]": $P = 0.0010$ for L-VR vs. R-VR before injection, $P = 0.2654$ for L-VR vs. R-VR after injection, $P = 0.0009$ for before vs. after injection in L-VR, $P = 0.0026$ for before vs. after injection in R-VR). $*P < 0.05$, $**P < 0.01$, $***P < 0.001$. n.s., no statistical significance.

preparation was pinned down in a transparent cooling chamber, continuously perfused with artificial cerebrospinal fluid (aCSF) at 6–8 °C, placed ∼15 cm high so that one of the eyes was facing the center of a computer screen (17-in LCD monitor, 1704FPVs; Dell) placed in a lateral position at a distance ∼30 cm from the preparation (40).

The different visual stimuli were written in MATLAB using the Psychophysics Toolbox extensions (50, 51), and a Master-8 programmable pulse generator (AMP Instruments) was used to coordinate the visual stimuli on the screen with the electrophysiological acquisition software pClamp (version 9.2).

All experiments were carried out in darkness, so that the only source of light was the computer screen, and before each experiment, the preparation was left to adapt for at least 30 min with a screen showing the background color (40).

Visual stimulation consisted of dots growing on the screen with different expansion rates (looming) or a vertical bar moving from rostral to caudal, or from caudal to rostral, with respect to the animal (with a total stimulus duration in both cases of 2.1 s). The default color (a black object on a white background) and other features were chosen because of their effectiveness to evoke ventral root responses (40). For the brightness adjustment, we calculated brightness with the luma formula $Y' = 0.299\ r + 0.587\ g + 0.114\ b$ (r, g, and b are standard RGB [sRGB] coordinates), according to International Telecommunication Union-Radiocommunication (ITU-R) BT.601 standard (52).

For recording bilateral neural activity in the ventral roots of the rostral spinal cord, suction electrodes made from borosilicate glass (Hilgenberg GmbH) using a vertical puller (Model PP-830; Narishige) filled with aCSF were used, connected to a 4-channel MA 102 amplifier (Elektroniklabor, Zoologie, University of Cologne, Germany). To avoid false-negative results, we stimulated the optic tectum using electrical microstimulation to ensure that activity was evoked in both ventral roots. Extracellular activity of the tectum and reticulospinal neurons was recorded using tungsten microelectrodes (∼1–5 MΩ) connected to a 4-channel MA 102 amplifier and a MA 103 preamplifier (Elektroniklabor, Zoologie, University of Cologne, Germany). For intracellular recordings of reticulospinal neurons, MRRN neurons were impaled with microelectrodes (resistance of 25–70 MΩ) filled with 3 M potassium acetate (KAc) and 0.1 M KCl. For all electrophysiological recordings, signals were digitized at 20 kHz using pClamp (version 10.2) software.

Drug Application. During electrophysiological recordings, the glutamate receptor antagonist kynurenic acid (2–4 mM; Sigma–Aldrich), the NMDA antagonist AP5 (0.5 mM; Tocris), the AMPA receptor antagonist NBQX (0.1 mM; Tocris), the $GABA_A$ receptor antagonist gabazine (0.1–1 mM; Tocris), the GABA agonist muscimol (1 mM; Sigma–Aldrich), or the sodium channel blocker TTX (3 μM; Sigma–Aldrich) was locally applied in the regions of interest (the optic tectum or MRRN) by pressure injection through a micropipette fixed to a holder, which was attached to a Picospritzer-II Microinjection Dispense System (Parker). The injected solution contained Fast Green dye to aid visualization of the injection spread. The holder was connected to an MP-285 motorized micromanipulator connected to a rotary optical encoder (ROE-200) through an MPC-200 controller (Sutter Instruments) so that the position of the pipette could be monitored to ensure precise drug injections in the regions of interest.

Quantification and Statistical Analysis. For all electrophysiological recordings, data analysis was performed using custom-written functions in MATLAB. We used

Downloaded at Palestinian Territory, occupied on November 26, 2021
www.manaraa.com

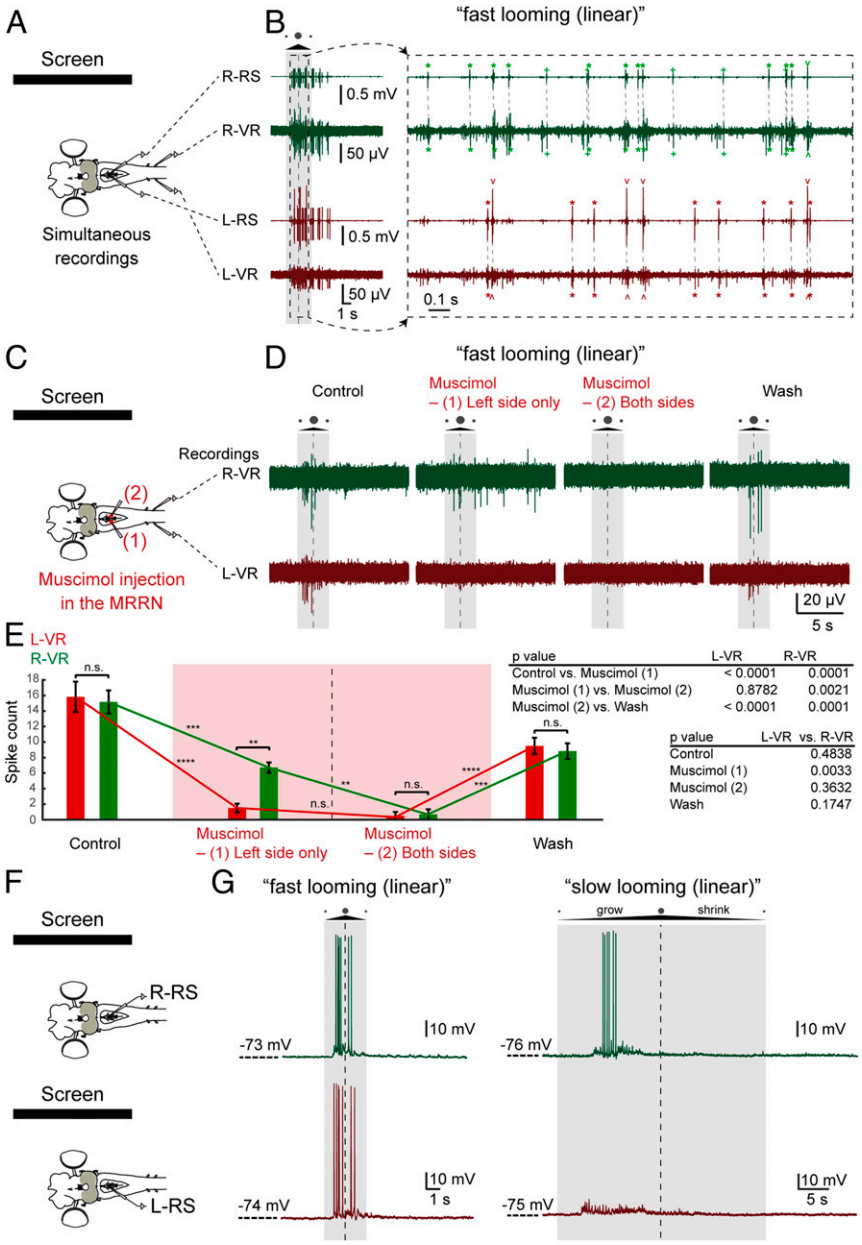

Fig. 8. Reticulospinal control of visual responses. (*A*) Simultaneous recordings from left (L) or right (R) reticulospinal neurons (RSs) and ventral roots (VRs). (*B*) When "fast looming (linear)" visual stimuli were applied, burst responses on both sides from reticulospinal neurons, as well as ventral roots, were observed (*Left*) with firing correlation between reticulospinal neurons and ventral roots on the respective sides (*Right*, smaller time scale). Correlated neural activity between reticulospinal neurons and ventral roots is shown with asterisks (*), regular/inverted caret (^), and plus (+) signs. The duration of the stimulus and the moment of maximum expansion are indicated by a shaded area and a vertical dotted line, respectively. (*C*) Sequential muscimol injection in the left and right MRRN. (*D*) After the first muscimol injection (left MRRN), L-VR activity was selectively inactivated, followed by total inactivation of ventral root activity after the subsequent second injection (right MRRN). (*E*) This observation is supported by the statistical analysis comparing average spike counts (of 7 trials) from the L-VR and R-VR between control (before muscimol injection) and first injection, first and second injection, and second injection and washout. Data are represented as mean ± SEM ($^{**}P < 0.01$, $^{***}P < 0.001$, $^{****}P < 0.0001$). n.s., no statistical significance. (*F*) Intracellular recordings of reticulospinal neurons in the left and right MRRN. (*G*, *Left*) Reticulospinal neurons on both the left and right sides were responsive to "fast looming (linear)" stimuli. (G, *Right*) All "fast looming" stimuli-responsive neurons on the right side also responded to the "slow looming (linear)" stimuli ($n = 6$ of 6), whereas neurons on the left side rarely responded to this type of stimuli ($n = 2$ of 7).

modified scripts from Daniel Wagenaar's Marine Biological Laboratory course package (2008–2011) (http://www.its.caltech.edu/~daw/teach.html) for the spike detection (which includes both single- and multiunit responses) and made spike raster plots accumulating different trials. Then, we calculated firing rates by constructing PSTHs.

For statistical analysis, we used 2-sample *t* tests or the Wilcoxon rank sum test for unpaired samples, paired *t* tests or the Wilcoxon signed-rank test for paired samples, and 1-way ANOVA tests (Friedman's test) for multiple samples in MATLAB. Throughout the figures, sample statistics are expressed as means ± SEMs. Statistical significance is shown as follows: n.s. (no statistical significance), $^{*}P < 0.05$, $^{**}P < 0.01$, $^{***}P < 0.001$, $^{****}P < 0.0001$.

ACKNOWLEDGMENTS. We thank Dr. Brita Robertson for valuable comments on the manuscript and encouragement throughout this study. This work is supported by a Japan Society for the Promotion of Science Overseas Research Fellowship (to D.G.S.), Swedish Medical Research Council Grants VR-M-K2013-62X-03026 and VR-M-2015-02816, Human Brain Project (funded from the European Union Seventh Framework Programme [FP7/2007-2013] under Grant Agreement 604102), European Union's Horizon 2020 Framework Programme for Research and Innovation under the Specific Grant Agreement nos. 720270 (Human Brain Project SGA1) and 785907 (Human Brain Project SGA2), the Parkinsonfonden, and the Karolinska Institutet's research funds.

1. J. D. Cohen, M. A. Castro-Alamancos, Neural correlates of active avoidance behavior in superior colliculus. *J. Neurosci.* **30**, 8502–8511 (2010).
2. J. H. Kaas, Topographic maps are fundamental to sensory processing. *Brain Res. Bull.* **44**, 107–112 (1997).
3. R. J. Krauzlis, L. P. Lovejoy, A. Zénon, Superior colliculus and visual spatial attention. *Annu. Rev. Neurosci.* **36**, 165–182 (2013).
4. D. Northmore, "The optic tectum." *The Encyclopedia of Fish Physiology: From Genome to Environment*, A. Farrell, Ed. (Academic Press, 2011), pp. 131–142.
5. A. B. Butler, Evolution of brains, cognition, and consciousness. *Brain Res. Bull.* **75**, 442–449 (2008).
6. S. Kumar, S. B. Hedges, A molecular timescale for vertebrate evolution. *Nature* **392**, 917–920 (1998).
7. D. G. Suzuki, Y. Murakami, H. Escriva, H. Wada, A comparative examination of neural circuit and brain patterning between the lamprey and amphioxus reveals the evolutionary origin of the vertebrate visual center. *J. Comp. Neurol.* **523**, 251–261 (2015).

Downloaded at Palestinian Territory, occupied on November 26, 2021
www.manaraa.com

8. D. G. Suzuki, Y. Murakami, Y. Yamazaki, H. Wada, Expression patterns of *Eph* genes in the "dual visual development" of the lamprey and their significance in the evolution of vision in vertebrates. *Evol. Dev.* **17**, 139–147 (2015).
9. T. C. Lacalli, New perspectives on the evolution of protochordate sensory and locomotory systems, and the origin of brains and heads. *Philos. Trans. R. Soc. Lond. B Biol. Sci.* **356**, 1565–1572 (2001).
10. T. E. Feinberg, J. M. Mallatt, *The Ancient Origins of Consciousness: How the Brain Created Experience* (MIT Press, 2016).
11. D. G. Suzuki, S. Grillner, The stepwise development of the lamprey visual system and its evolutionary implications. *Biol. Rev. Camb. Philos. Soc.* **93**, 1461–1477 (2018).
12. M. R. Jones, S. Grillner, B. Robertson, Selective projection patterns from subtypes of retinal ganglion cells to tectum and pretectum: Distribution and relation to behavior. *J. Comp. Neurol.* **517**, 257–275 (2009).
13. K. Saitoh, A. Ménard, S. Grillner, Tectal control of locomotion, steering, and eye movements in lamprey. *J. Neurophysiol.* **97**, 3093–3108 (2007).
14. A. A. Kardamakis, K. Saitoh, S. Grillner, Tectal microcircuit generating visual selection commands on gaze-controlling neurons. *Proc. Natl. Acad. Sci. U.S.A.* **112**, E1956–E1965 (2015).
15. A. A. Kardamakis, J. Pérez-Fernández, S. Grillner, Spatiotemporal interplay between multisensory excitation and recruited inhibition in the lamprey optic tectum. *eLife* **5**, e16472 (2016).
16. F. M. Ocaña *et al*., The lamprey pallium provides a blueprint of the mammalian motor projections from cortex. *Curr. Biol.* **25**, 413–423 (2015).
17. M. Stephenson-Jones, E. Samuelsson, J. Ericsson, B. Robertson, S. Grillner, Evolutionary conservation of the basal ganglia as a common vertebrate mechanism for action selection. *Curr. Biol.* **21**, 1081–1091 (2011).
18. A. K. Kozlov, A. A. Kardamakis, J. Hellgren Kotaleski, S. Grillner, Gating of steering signals through phasic modulation of reticulospinal neurons during locomotion. *Proc. Natl. Acad. Sci. U.S.A.* **111**, 3591–3596 (2014).
19. G. De Franceschi, T. Vivattanasarn, A. B. Saleem, S. G. Solomon, Vision guides selection of freeze or flight defense strategies in mice. *Curr. Biol.* **26**, 2150–2154 (2016).
20. J. M. Ache *et al*., Neural basis for looming size and velocity encoding in the Drosophila giant fiber escape pathway. *Curr. Biol.* **29**, 1073–1081.e4 (2019).
21. C. Shang *et al*., Divergent midbrain circuits orchestrate escape and freezing responses to looming stimuli in mice. *Nat. Commun.* **9**, 1232 (2018).
22. I. Temizer, J. C. Donovan, H. Baier, J. L. Semmelhack, A visual pathway for looming-evoked escape in larval zebrafish. *Curr. Biol.* **25**, 1823–1834 (2015).
23. T. O. Helmbrecht, M. Dal Maschio, J. C. Donovan, S. Koutsouli, H. Baier, Topography of a visuomotor transformation. *Neuron* **100**, 1429–1445.e4 (2018).
24. S. Grillner, Biological pattern generation: The cellular and computational logic of networks in motion. *Neuron* **52**, 751–766 (2006).
25. T. Wannier, T. G. Deliagina, G. N. Orlovsky, S. Grillner, Differential effects of the reticulospinal system on locomotion in lamprey. *J. Neurophysiol.* **80**, 103–112 (1998).
26. T. G. Deliagina, P. V. Zelenin, P. Fagerstedt, S. Grillner, G. N. Orlovsky, Activity of reticulospinal neurons during locomotion in the freely behaving lamprey. *J. Neurophysiol.* **83**, 853–863 (2000).
27. S. Grillner *et al*., Modeling a vertebrate motor system: Pattern generation, steering and control of body orientation. *Prog. Brain Res.* **165**, 221–234 (2007).
28. I. C. Zompa, R. Dubuc, A mesencephalic relay for visual inputs to reticulospinal neurones in lampreys. *Brain Res.* **718**, 221–227 (1996).
29. I. C. Zompa, R. Dubuc, Diencephalic and mesencephalic projections to rhombencephalic reticular nuclei in lampreys. *Brain Res.* **802**, 27–54 (1998).
30. L. Capantini, A. von Twickel, B. Robertson, S. Grillner, The pretectal connectome in lamprey. *J. Comp. Neurol.* **525**, 753–772 (2017).
31. F. Ullén, T. G. Deliagina, G. N. Orlovsky, S. Grillner, Visual pathways for postural control and negative phototaxis in lamprey. *J. Neurophysiol.* **78**, 960–976 (1997).
32. A. Nieder, E. K. Miller, Coding of cognitive magnitude: Compressed scaling of numerical information in the primate prefrontal cortex. *Neuron* **37**, 149–157 (2003).
33. S. Dehaene, The neural basis of the Weber-Fechner law: A logarithmic mental number line. *Trends Cogn. Sci. (Regul. Ed.)* **7**, 145–147 (2003).
34. B. Fritzsch, "Ontogenetic clues to the phylogeny of the visual system." in *The Changing Visual System*, P. Bagnoli, W. Hodos, Eds. (Plenum Press, 1991), pp. 33–49.
35. D. G. Suzuki *et al*., Comparative morphology and development of extra-ocular muscles in the lamprey and gnathostomes reveal the ancestral state and developmental patterns of the vertebrate head. *Zoological Lett.* **2**, 10 (2016).
36. J. P. Rio *et al*., Presumptive GABAergic centrifugal input to the lamprey retina: A double-labeling study with axonal tracing and GABA immunocytochemistry. *Brain Res.* **600**, 9–19 (1993).
37. J. P. Rio *et al*., Retinal and non-retinal inputs upon retinopetal RMA neurons in the lamprey: A light and electron microscopic study combining HRP axonal tracing and GABA immunocytochemistry. *J. Chem. Neuroanat.* **12**, 51–70 (1996).
38. J. P. Rio, J. Repérant, N. P. Vesselkin, N. B. Kenigfest-Rio, D. Miceli, Dual innervation of the lamprey retina by GABAergic and glutamatergic retinopetal fibers. A quantitative EM immunogold study. *Brain Res.* **959**, 336–342 (2003).
39. J. Pérez-Fernández, M. Stephenson-Jones, S. M. Suryanarayana, B. Robertson, S. Grillner, Evolutionarily conserved organization of the dopaminergic system in lamprey: SNc/VTA afferent and efferent connectivity and D2 receptor expression. *J. Comp. Neurol.* **522**, 3775–3794 (2014).
40. J. Pérez-Fernández, A. A. Kardamakis, D. G. Suzuki, B. Robertson, S. Grillner, Direct dopaminergic projections from the SNc modulate visuomotor transformation in the lamprey tectum. *Neuron* **96**, 910–924.e5 (2017).
41. S. P. Collin, W. L. Davies, N. S. Hart, D. M. Hunt, The evolution of early vertebrate photoreceptors. *Philos. Trans. R. Soc. Lond. B Biol. Sci.* **364**, 2925–2940 (2009).
42. Y. Shichida, T. Matsuyama, Evolution of opsins and phototransduction. *Philos. Trans. R. Soc. Lond. B Biol. Sci.* **364**, 2881–2895 (2009).
43. T. D. Lamb, Evolution of phototransduction, vertebrate photoreceptors and retina. *Prog. Retin. Eye Res.* **36**, 52–119 (2013).
44. S. Asteriti, S. Grillner, L. Cangiano, A Cambrian origin for vertebrate rods. *eLife* **4**, e07166 (2015).
45. O. S. E. Gustafsson, S. P. Collin, R. H. H. Kröger, Early evolution of multifocal optics for well-focused colour vision in vertebrates. *J. Exp. Biol.* **211**, 1559–1564 (2008).
46. V. I. Govardovskii, D. V. Lychakov, Visual cells and visual pigments of the lamprey, Lampetra fluviatilis. *J. Comp. Physiol. A* **154**, 279–286 (1984).
47. A. J. Barker, H. Baier, Sensorimotor decision making in the zebrafish tectum. *Curr. Biol.* **25**, 2804–2814 (2015).
48. A. B. Butler, W. Hodos, *Comparative Vertebrate Neuroanatomy: Evolution and Adaptation* (Wiley-Interscience, ed. 2, 2005).
49. Institute of Laboratory Animal Research; National Research Council, *Guide for the Care and Use of Laboratory Animals* (National Academy Press, 1996).
50. D. H. Brainard, The psychophysics toolbox. *Spat. Vis.* **10**, 433–436 (1997).
51. D. G. Pelli, The VideoToolbox software for visual psychophysics: Transforming numbers into movies. *Spat. Vis.* **10**, 437–442 (1997).
52. S. Bezryadin, P. Bourov, D. Ilinih, "Brightness calculation in digital image processing." in *International Symposium on Technologies for Digital Photo Fulfillment* (Society for Imaging Science and Technology, Las Vegas, NV, 2007), vol. 1, pp. 10–15.

Downloaded at Palestinian Territory, occupied on November 26, 2021

www.manaraa.com